Original Research

Thapsigargin affects presenilin-2 but not presenilin-1 regulation in SK-N-BE cells

Roberto Rivabene, Sergio Visentin, Paola Piscopo, Chiara De Nuccio, Alessio Crestini, Francesca Svetoni, Paolo Rosa and Annamaria Confaloni

Department of Cell Biology and Neuroscience, Istituto Superiore di Sanità, Viale Regina Elena, 299 00161 Rome, Italy
Corresponding author: Annamaria Confaloni. Email: annamaria.confaloni@iss.it

Abstract

Presenilin-1 (PS1) and presenilin-2 (PS2) are transmembrane proteins widely expressed in the central nervous system, which function as the catalytic subunits of γ-secretase, the enzyme that releases amyloid-β protein (Aβ) from ectodomain cleaved amyloid precursor protein (APP) by intramembrane proteolysis. Mutations in PS1, PS2, and Aβ protein precursor are involved in the etiology of familial Alzheimer's disease (FAD), while the cause of the sporadic form of AD (SAD) is still not known. However, since similar neuropathological changes have been observed in both FAD and SAD, a common pathway in the etiology of the disease has been suggested. Given that age-related deranged Ca^{2+} regulation has been hypothesized to play a role in SAD pathogenesis via PS gene regulation and γ-secretase activity, we studied the *in vitro* regulation of PS1 and PS2 in the human neuron-like SK-N-BE cell line treated with the specific endoplasmic reticulum (ER) calcium ATPase inhibitor Thapsigargin (THG), to introduce intracellular Ca^{2+} perturbations and mimic the altered Ca^{2+} homeostasis observed in AD. Our results showed a consistent and significant down-regulation of PS2, while PS1 appeared to be unmodulated. These events were accompanied by oxidative stress and a number of morphological alterations suggestive of the induction of apoptotic machinery. The administration of the antioxidant *N*-acetylcysteine (NAC) did not revert the THG-induced effects reported, while treatment with the Ca^{2+}-independent ER stressor Brefeldin A did not modulate basal PS1 and PS2 expression. Collectively, these results suggest that Ca^{2+} fluctuation rather than ER stress and/or oxidative imbalance seems to play an essential role in PS2 regulation and confirm that, despite their strong homology, PS1 and PS2 could play different roles in AD.

Keywords: Alzheimer's disease, apoptosis, calcium, neurodegeneration, oxidative stress, presenilins

***Experimental Biology and Medicine* 2014; 239: 213–224. DOI: 10.1177/1535370213514317**

Introduction

Alzheimer's disease (AD), one of the most common types of dementia, is a late-onset brain disorder affecting the elderly that is clinically characterized by memory loss, impairment of cognitive function, and changes in behavior and personality.[1] The neuropathological hallmarks of AD are the formation of two main protein aggregates: senile plaques and neurofibrillary tangles, both of which are involved in progressive neuronal degeneration and death.[2] Senile plaques are characterized by the β-amyloid peptide (Aβ) deposition in the human brain, a 39–43 amino acid peptide derived from the proteolytic cleavage of the amyloid precursor protein (APP) via the amyloidogenic (Aβ forming) pathway.[1,3] This route is driven by a complex of presenilins (PSs), Nicastrin, Anterior Pharynx Defective 1, and Presenilin Enhancer-2 (PEN-2), formally known as the γ-secretase complex, a membrane protein complex regulating the transmembranous proteolysis of APP.[4]

Both presenilin-1 (PS1) and presenilin-2 (PS2) are multipass membrane proteins, widely expressed in the central nervous system and peripheral tissues, which show a remarkable homology in the sequence of genes, transcripts, and proteins.[5] Their full-length proteins, highly unstable, are cleaved into two stable pieces, a N-terminal fragment (NTF) and a C-terminal fragment (CTF) which represent the functional active forms of PSs.[6] Several mutations in PS1, PS2, and APP are involved in the etiology of familial AD (FAD), while the cause of the sporadic form of AD (SAD), which represents the majority of cases occurring at late age, is still not known. However, the neuropathological changes in both FAD and SAD are similar, suggesting that they share a common pathway in the etiology of the disease.[7] Like FAD, SAD is thought to be caused by the accumulation of

the Aβ peptide, which occurs as a consequence of poorly understood complex biological and environmental interactions. In this context, it has been reported that changes in calcium levels and dynamics alter the metabolism and production of the pathological proteins associated with the disease, Aβ and the microtubule-associated protein tau.[8] At the same time, downstream events from both Aβ and tau accumulation may exacerbate Ca^{2+} dysregulation, suggesting a possible loop mechanism involving the disruption of Ca^{2+} homeostasis, apoptosis, and alterations in APP processing.[9] It should be noted that dysregulation of intracellular Ca^{2+} homeostasis occurs at the ultimate stage of essentially all forms of cell death. Thus, the mechanisms that regulate intracellular Ca^{2+} metabolism are critical for the maintenance of cell survival.

Basal Ca^{2+} levels are fine-tuned by a number of calcium pumps and binding proteins, which remove free cytosolic calcium so as to maintain a resting low concentration of the divalent cation in the cytoplasm. Calcium enters the cytosol from the extracellular space, through voltage-dependent and receptor-operated ion channels, including glutamate receptors such as the α-amino-3-hydroxy-5-methyl-4-isoxazolepropionic acid (AMPA) and N-methyl-D-aspartate (NMDA) receptors. Calcium can also enter the cytosol from intracellular stores. Virtually all intracellular compartments participate in the homeostasis of the ion and its intracellular movement between compartments. Among these, the endoplasmic reticulum (ER) plays a pivotal role, being the largest intracellular reservoir of Ca^{2+} and being capable of releasing the ion following the activation of metabotropic plasmalemmal receptors, and the opening of ryanodine (RyRs) or inositol (1,4,5)-trisphosphate (IP3Rs)-sensitive receptors located in the ER membranes. On the contrary, the recovery of low cytosolic Ca^{2+} is achieved via a multitude of ATP-dependent Ca^{2+} pump exchange mechanisms present on the plasma membrane (e.g., Na/Ca^{2+} exchange) and intracellular membranes, the main ones being in the mitochondria and ER.[8] The sarco-endoplasmic reticulum Ca^{2+} ATPase (SERCA), the main player in Ca^{2+} re-uptake in the ER after Ca^{2+} release, deserves a special mention in this context.

Much attention has been given to the fact that some FAD-linked PS mutants cause the dysregulation of cellular Ca^{2+} homeostasis via the altered expression or sensitivity of both RyRs and IP3Rs ion channels[10,11] and of SERCA pumps,[12,13] indicating that wild-type PSs may also play a specific role in Ca^{2+} homeostasis.[14,15] Finally, both PS2 NTF and CTF have been shown to be physically associated with both IP3Rs and RyRs via the Ca^{2+}-binding protein sorcin.[16,17]

Several studies have reported that PS expression in the human brain is widespread and primarily neuronal, with decreased PS1 and PS2 mRNA levels in SAD.[18,19] However, a number of investigations did not support these findings, leaving the question relatively unresolved.[20] Thus, at present, it remains unclear whether PS expression levels are altered in SAD.

Considerable evidence supports a cause–effect relationship among altered Ca^{2+} homeostasis, oxidative stress, ER stress, and neuronal dysfunction and apoptotic cell death in several neurodegenerative disorders, including AD.[21] For example, it has been reported that AD-associated mutations of PS1 disrupt Ca^{2+} homeostasis and increase susceptibility to ER stress and apoptosis,[22,23] whereas wild-type PS1 is necessary for cellular responses to ER stress.[24] Furthermore, an AD-associated splice variant of PS2 increases vulnerability to ER stress.[25] Impaired ER function is considered an important factor in the neuropathology of a wide variety of neurological disorders.[26–28] Studies related to AD have shown that the neurotoxic effects of the amyloid β-peptide are at least partially targeted to the ER.[29,30] Because the ER is a central site of protein folding, ER stress can lead to increased intracellular levels of misfolded proteins, and eventual cell death by apoptosis, processes that may contribute to neurodegenerative disorders.[31]

There is a growing body of evidence supporting the idea that brain aging is associated with a progressive imbalance between antioxidant defenses and the intracellular concentration of reactive oxygen species (ROS).[32,33] The possibility that the age-related oxidative shift in redox status may cause subpathological changes in calcium homeostasis has also been reported.[34] In view of these facts and also given that both Ca^{2+} homeostasis alterations and oxidative imbalance have been proposed as factors that may influence PS gene transcription and γ-secretase activity,[35] we planned an *in vitro* investigation to explore the relationship between Ca^{2+} perturbation, oxidative stress, and PS expression and regulation. Our results show that the rapid and persistent increase in cytosolic Ca^{2+}, but not ER stress and redox imbalance, seems to correlate with PS1 and PS2 differently both at the transcriptional and post-transcriptional level.

Methods

Cell culture

Human neuroblastoma cell line SK-N-BE (kindly supplied by Prof G. Poiana, University ''La Sapienza,'' Rome, Italy) was cultivated in RPMI-1640 medium (Euroclone) supplemented with 10% heat-inactivated (v/v) fetal bovine serum (FBS), 5 mM L-glutamine, penicillin (100 IU/mL), and streptomycin (100 μg/mL). Cell cultures were maintained at 37°C in a humidified atmosphere of 5% CO_2. For the experiments, the cells were seeded at a density of $1 \times 10^4/cm^2$ on 60-mm plastic culture dishes and were grown to 80% confluence.

Cell treatments

We used Thapsigargin (THG, Sigma, St. Louis, MO), a sesquiterpene alkaloid that poisons SERCA[36] to introduce a rapid and persistent rise in intracytosolic Ca^{2+} within cells. THG was added to the medium from a stock solution of 1 mM in dimethyl sulfoxide (DMSO) to a final working concentration of 1 μM. This concentration, which was chosen on the basis of initial experiments in which we established the optimal working concentration and incubation periods for the induction of apoptosis without affecting significantly the viability of cells (data not shown), is in line with that previously reported by others[12,37,38] and our group.[39] To introduce ER stress without Ca^{2+} mobilization, Brefeldin A (Sigma, St. Louis, MO) was added to the

medium from a stock solution of 5 mg/mL in DMSO to a final working concentration of 5 μg/mL.[40] Where appropriate, cells treated with the same volume of DMSO were used as a control. To introduce alterations in the redox profile of the cells, L-buthionine-[S,R]-sulfoximine (BSO, Sigma, St. Louis, MO) and *N*-acetylcysteine (NAC, Sigma, St. Louis, MO) were added directly to the culture medium at concentrations of 100 μM and 5 mM, respectively. With regard to the BSO and NAC concentrations used in this work, our purpose was to induce consistent and significant alterations of cell redox potential without affecting cell viability, structure, and function. In view of these facts, both of the BSO and NAC concentrations were accurately selected on the basis of specific preliminary experiments (data not shown) and are in line with those used by other groups to elicit their respective effects in neuroblastoma cell lines.[41,42] At each endpoint selected, cells were harvested by trypsinization and processed as described below. The general morphology of cell monolayers, before and after treatment, was monitored by light microscopy.

Ca^{2+} videoimaging

Neuroblastoma cells to be used for Ca^{2+} recording were seeded on uncoated glass coverslips and kept in growth media for 24/48 h prior to recording. Fura-2-AM was dissolved in a solution composed of DMSO and pluronic acid (20%) and sonicated for 5 min at 35°C, to obtain a 1 mM stock solution. To obtain the loading medium, Fura-2-AM was further dissolved to 1 μM in the experimental saline solution with the following composition (mM): 140 NaCl, 5 KCl, 2.5 $CaCl_2$, 1 $MgCl_2$, 10 glucose, and 10 Hepes (pH 7.4). The cells were kept for 50 min in the loading medium, then washed carefully and left for a further 20–30 min before recording, to allow for complete hydrolysis of the AM. Glass coverslips bearing Fura-2-AM-loaded cells were transferred to a recording chamber on the stage of a Zeiss Axiovert 135 inverted microscope. In addition to a bulk perfusion system, a local perfusion system allowed the fast and localized flow of solution only on the cells studied (Rapid Solution Exchange 100; Biologic, France). To excite Fura-2, the appropriate light wavelengths (340/380 nm) were produced by a monochromator (Polychrome II, Till Photonics), conveyed along an optic fiber to a dichroic mirror (filter) and finally to the Fura-2-loaded cells. Light emission at 510 nm was collected by a charged-coupled device (CCD) cooled digital camera (Sensicam; PCO) and recorded on the memory of a PC computer. A dedicated software package (Imaging Workbench 6.0; Indec Biosystems; USA) enabled control of the experimental recording and of the first phase of data analysis. For further data analysis and graphic presentation Origin 7.5 (Origin Lab) was utilized. Ca^{2+} concentrations are represented as the ratio between the emissions at 340 and 380 nm (ratio 340/380).

Measurement of cell growth

Cells were cultured in duplicate in 60-mm dishes starting at an initial density of $1 \times 10^4/cm^2$. Twenty-four hours after seeding, 1 μM THG was added, and the cells were grown for 24 h in the absence or presence of DMSO, used as a control for THG. DMSO (0.1%) did not affect the proliferation of the cells. For counting, the cells were detached after a previous washing with phosphate-buffered saline (PBS), followed by a 10-min exposure at 37°C to a solution of 0.05% Trypsin in PBS (pH 7.2), and were then suspended to give a single cell suspension. Cell proliferation was followed by counting the total number of cells in each flask using a haematocytometer chamber. Cell viability was determined using the 0.4% Trypan blue dye exclusion test. The number of cells detached from the substrate and freely floating in the cell medium was also evaluated.

Lactate dehydrogenase release assay

We analyzed the total amounts of lactate dehydrogenase (LDH) in the culture medium by a LDH Cytotoxicity Detection Kit (Takara, Tokyo, Japan) in accordance with the manufacturer's instructions, to measure the cytotoxicity induced by THG treatment. Briefly, after each incubation time of the cells with THG, the culture medium was collected and incubated for 30 min at room temperature with the reaction mixture provided. The reaction mixture was then mixed with 1 N HCl, and the absorbance measured at a wavelength of 490 nm was considered to represent the amount of LDH released.

RNA isolation and realtime polymerase chain reaction

Total RNA was extracted from untreated and treated SK-N-BE cells (Invisorb SpinCell RNA, Invitek) and retrotranscribed into cDNA using a SuperScript III first-strand cDNA synthesis kit (Invitrogen Inc., Carlsbad, CA) with random primers, according to the manufacturer's protocol. Reverse transcription quantitative realtime polymerase chain reaction (RT-qPCR) was performed using the ABI PRISM 7000 Sequence Detection System (Applied Biosystems, Foster City, USA) with the TaqMan Universal PCR Master Mix and TaqMan Gene expression assays (Applied Biosystems). The parameters for PCR amplification were 50°C for 2 min, 95°C for 10 min followed by 40 cycles of 95°C for 15 s and 60°C for 1 min. The PCRs were performed in triplicate for each sample, and 18 S rRNA was chosen as the reference gene. The relative expression of mRNA was calculated using the comparative Ct method.

Evaluation of apoptosis

Apoptosis was evaluated both in adherent and detached cells using the Terminal deoxynucleotidyl transferase dUTP nick end labeling (TUNEL) and 4′,6-diamidino-2-phenylindole-2-HCl (DAPI) chromatin staining techniques, respectively. The TUNEL method identifies apoptotic cells *in situ* by using terminal deoxynucleotidyl transferase (TdT) to transfer biotin-dUTP to the strand breaks of cleaved DNA. The biotin-labeled cleavage sites are then detected by reaction with horseradish peroxidase (HRP)-conjugated streptavidin and visualized by diaminobenzidine (DAB), showing a brown color. For TUNEL staining, a commercially available kit (Promega) was used. Adherent cells were washed in PBS, fixed with 4% formaldehyde in PBS

for 10 min, and then processed following the suggested experimental procedures. For DAPI staining, detached cells were collected by centrifugation, washed in PBS, and fixed with 4% formaldehyde in PBS for 10 min at room temperature. After washing in the same buffer, cells were stained with the chromatin dye DAPI for 10 min at 37°C. After washing in PBS, all samples were seeded in glass coverslips previously coated with polylysine and mounted with a liquid-mounting medium. All observations were made with a Carl-Zeiss fluorescence photomicroscope.

Evaluation of oxidative stress

The enzymatic activity of superoxide dismutase (SOD) was detected as previously described.[43] SOD was determined by quantification of pyrogallol auto oxidation inhibition and the results were expressed as units/mg protein. One unit of enzyme activity was defined as the amount of enzyme necessary for inhibiting the reaction by 50%. Auto oxidation of 0.2 mM pyrogallol in air-equilibrated 50 mM Tris-cacodylic acid buffer, pH 8.2, containing 1 mM diethylenetriaminepentaacetic acid was measured by an increase in absorbance at 420 nm. To determine the total intracellular glutathione (GSH) content, an enzymatic recycling assay with GSH reductase (type IV, Sigma) and 5,5′-dithiobis-2-nitrobenzoic acid (DTNB, Sigma) was used.[44] For the measurement of oxidized glutathione (GSSG), the acidified homogenates were submitted to derivatization with undiluted 2-vinylpyridine (Aldrich, Milwaukee, WI, USA) in the presence of triethanolamine (Sigma) for 1 h at room temperature. Samples were then assayed using the same procedure described above for total GSH measurement. The amount of reduced GSH present in the samples was calculated as the difference between total GSH and GSSG levels. The data were expressed as nmoles of GSH or GSSG per mg of cell protein.

Western blot analysis

Cells were harvested in lysis buffer (50 mM Tris, 150 mM NaCl, NP-40 10%, and Na-deoxycholate 10%), containing a cocktail of protease inhibitors (Sigma-Aldrich). Each sample containing 20 μg of protein was placed in sample buffer (0.5 M Tris–HCl pH 6.8, 10% glycerol, 2% (w/v) SDS, 5% (v/v) 2-β-mercaptoethanol, and 0.05% bromophenol blue), then denatured by boiling at 95 to 100°C for 5 min. The protein samples were resolved on 10% SDS–PAGE gels and transferred to polyvinylidene difluoride membranes (Westran, Schleicher and Schuell). The blots were first blocked with 5% nonfat powdered milk in Tris-buffered saline (TBS)/Tween 0.1% and then probed overnight at 4°C with one of the following primary antibodies: mouse monoclonal to PS2 (Abcam, cat. Ab15549, dil. 1:1.000, that recognizes the 20 kDa PS2 CTF); mouse monoclonal to PS2 (Abcam, cat. Ab15548, dil. 1:1.000, that recognizes both the 28 kDa PS2 NTF and 46 kDa full-length PS2); and mouse monoclonal anti-β-actin (Sigma-Aldrich, cat. A 5441, dil. 1:100.000). The membranes were then washed in TBS/Tween 0.1%, and incubated for 1 h at RT with HRP-conjugated antimouse secondary antibody (Chemicon, cat. 92590, 1:20.000). The blots were developed using Immun-Star™ WesternC™ (Bio-Rad Laboratories, Hercules, CA, cat. 170-5070) according to the manufacturer's instructions. Densitometric analysis was performed using an FX-Imager densitometer and the Quantity One software (Bio-Rad).

Protein content

The protein concentration was measured using the commercially available Coomassie brilliant blue dye-binding assay (Bio-Rad), according to the manufacturer's instructions. Bovine γ-globulin was used as a standard.

Statistical analysis

The data are expressed as mean ± standard error of mean (SEM). Comparisons among groups were made using Student's *t*-test or one-way analysis of variance (ANOVA) followed by Bonferroni's multiple comparison test, with significance set at $P < 0.05$.

Results

THG induces Ca^{2+} efflux from ER to cytosol

The (sesquiterpene lactone) tumor-promoting agent THG is known to bind and inhibit the SERCA, which acts by pumping cytoplasmic Ca^{2+} into the ER. Given this capability, THG is routinely used to induce intracellular Ca^{2+} rearrangement, consisting primarily of Ca^{2+} depletion from the ER and a rise in Ca^{2+} in the cytoplasmic compartment. To verify the effect of long-lasting (24 h) application of THG on intracellular Ca^{2+} pools in the human neuroblastoma cell line SK-N-BE, we employed a fluorescence videoimaging technique with the Ca^{2+} probe Fura-2. The cytoplasmic Ca^{2+} concentration recorded in THG-treated cells in the absence of any other exogenous stimulation (basal condition) was significantly higher than in untreated cells, probably due to a THG-induced ER Ca^{2+} translocation to the cytoplasm (Figure 1a). Two different strategies were utilized to evaluate the effect of long-lasting THG treatment on the ER Ca^{2+} pool: metabotropic receptor activation and acute application of THG in the absence of Ca^{2+} (THG/0-Ca^{2+}). In these cells, uridine diphosphate (UDP) is known to cause an IP3-dependent ER Ca^{2+} release by activating P2Y6 receptors.[45] As expected, the acute application of 100 μM UDP induced a rapid cytoplasmic Ca^{2+} build up in control cells, which slowly returned to the basal level. On the contrary, UDP was unable to affect cytoplasmic Ca^{2+} when applied to the cells after chronic treatment with THG, due to ER Ca^{2+} depletion after 24 h of treatment with THG (Figure 1b). To rule out a possible effect on receptor expression or function, the effect of acute application of THG/0-Ca^{2+} was evaluated in control and THG-treated cells (Figure 1c). In control cells, THG/0-Ca^{2+} caused a slow increase in Ca^{2+} followed by another larger increase in Ca^{2+} upon Ca^{2+} readmission, depicting Ca^{2+} movement from the ER to the cytoplasm and Ca^{2+} influx from capacitative channels opened by ER Ca^{2+} depletion. The nature of this latter phenomenon was confirmed by the sensitivity to the capacitative channel inhibitor SKF96395 (Figure 1d). A completely different effect was observed after chronic THG treatment: a

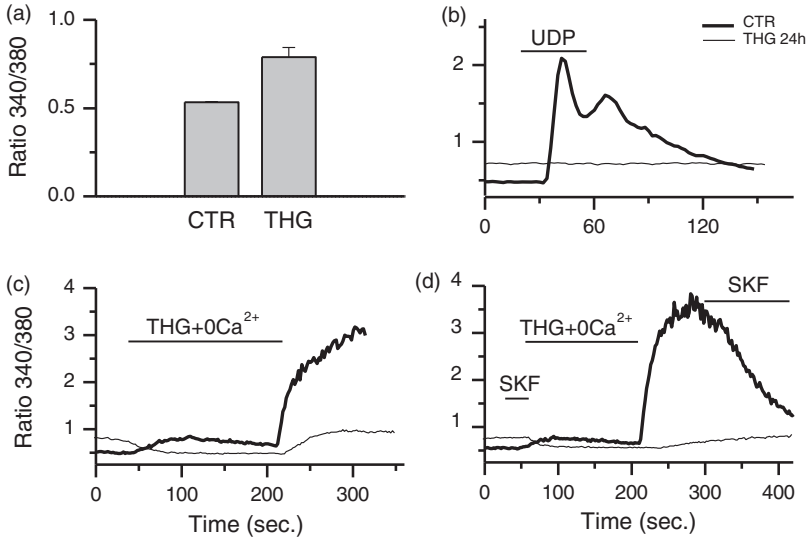

Figure 1 Effects of THG on intracellular Ca^{2+} in SK-N-BE cells. The effects of the chronic application (24 h) of THG were evaluated by fluorescence videoimaging in Fura-2-loaded cells. The basal Ca^{2+} level was recorded in untreated (CTR) and THG-treated cells in the absence of any exogenous stimulus. As shown in (a), THG induced a significant increase in the basal Ca^{2+} level. Two strategies were adopted to evaluate the effect of THG on ER Ca^{2+}: the application of the metabotropic agent UDP (b) and of THG itself in the absence of Ca^{2+} (c). The response to UDP and to the acute application of THG was abrogated by previous treatment with the SERCA inhibitor, depicting its effect on ER Ca^{2+} depletion. Moreover, when the store-operated channel (SOC) inhibitor SKF96395 was used, it abrogated the rise in Ca^{2+} due to Ca^{2+} readmission into CTR cells, but did not have any effect on THG-treated cells, depicting Ca^{2+} permeation through SOC channels in CTR but not in THG-treated cells (d).

decline in Ca^{2+}, probably due to Ca^{2+} transfer from the cytoplasm to the extracellular environment, and a lack of increase in Ca^{2+} upon Ca^{2+} readmission, probably due to desensitization of the capacitative channels. According to these data, long-lasting treatment with THG causes a rearrangement of the intracellular Ca^{2+} pools, consisting of a rise in cytoplasmic Ca^{2+} and ER Ca^{2+} depletion.

THG induces cell-growth arrest and morphological alterations, with an emerging picture of apoptosis

As can be observed in Figure 2(a), cell growth in the presence of 1 μM of THG was progressively impaired when compared to cells grown under normal conditions. In particular, significant reductions in the adherent cell number of about 20 and 27% were found, respectively, after 12 and 24 h of treatment. A parallel morphological analysis of THG-treated cell monolayers performed by phase contrast microscopy showed time-related emerging alterations which resulted, after 24 h of treatment, in a loss of neuritis, cell texture, and shape (Figure 2(c)), with respect to the controls (Figure 2(b)).

In view of these morphological alterations, we carried out a specific investigation into apoptosis. Apoptosis in adherent cells was characterized using TUNEL staining, while DAPI staining was used in detached cells. In comparison with the negative staining observed in control adherent cells (Figure 2(d)), cells exposed to 1 μM THG for 24 h contained condensed cellular chromatin (Figure 2(e)), as indicated by the strong and diffuse positive staining, which reflected the presence of both DNA fragmentation and chromatin condensation. A parallel analysis performed on the supernatants showed a clear increase in the number of cells freely floating in the medium, as a consequence of detachment from the substrate, in THG-treated samples (Figure 2(g)), with respect to controls (Figure 2(f)). In addition, several cells displaying apoptotic nuclear alterations, such as chromatin clumps as well as condensed nuclei with aggregated chromatin were also visible in THG-treated cells (Figure 2(g), arrows). Viability analysis of resting adherent cells evaluated using the Trypan blue exclusion test did not show any significant differences between THG-treated and untreated cells, with viability at 96%, whether only a modest nonsignificant increase in LDH released in the medium of THG-treated cells, if compared to controls, was detected.

THG induces the time-dependent down-regulation of PS2 but not PS1

To test the effect of altered Ca^{2+} homeostasis on the regulation of PS genes, we analyzed the SK-N-BE neuron-like cell transcripts by realtime PCR after 6, 12, and 24 h of THG treatment. As observed in Figure 3(b), a time-dependent decrease in PS2 transcripts was clearly evident after treatment, with a drop of 30% after 6 h of THG exposure with respect to the control conditions; this down-regulation was enhanced after 12 and 24 h of treatment, with a drop of 65 and 60%, respectively. Finally, THG treatment did not affect PS1 expression at all time points (Figure 3(a)). In view of the results obtained, a specific western blot analysis for PS2 was carried out. As shown in Figure 3(c), there was a consistent and significant reduction in both NTF and CTF at 6, 12, and 24 h after THG exposure. No band corresponding to the full-length form of PS2 has been detected, in line with data reported in the literature for which endogenous PSs holoprotein level is relatively low, being on the border line of detection.[15,46,47]

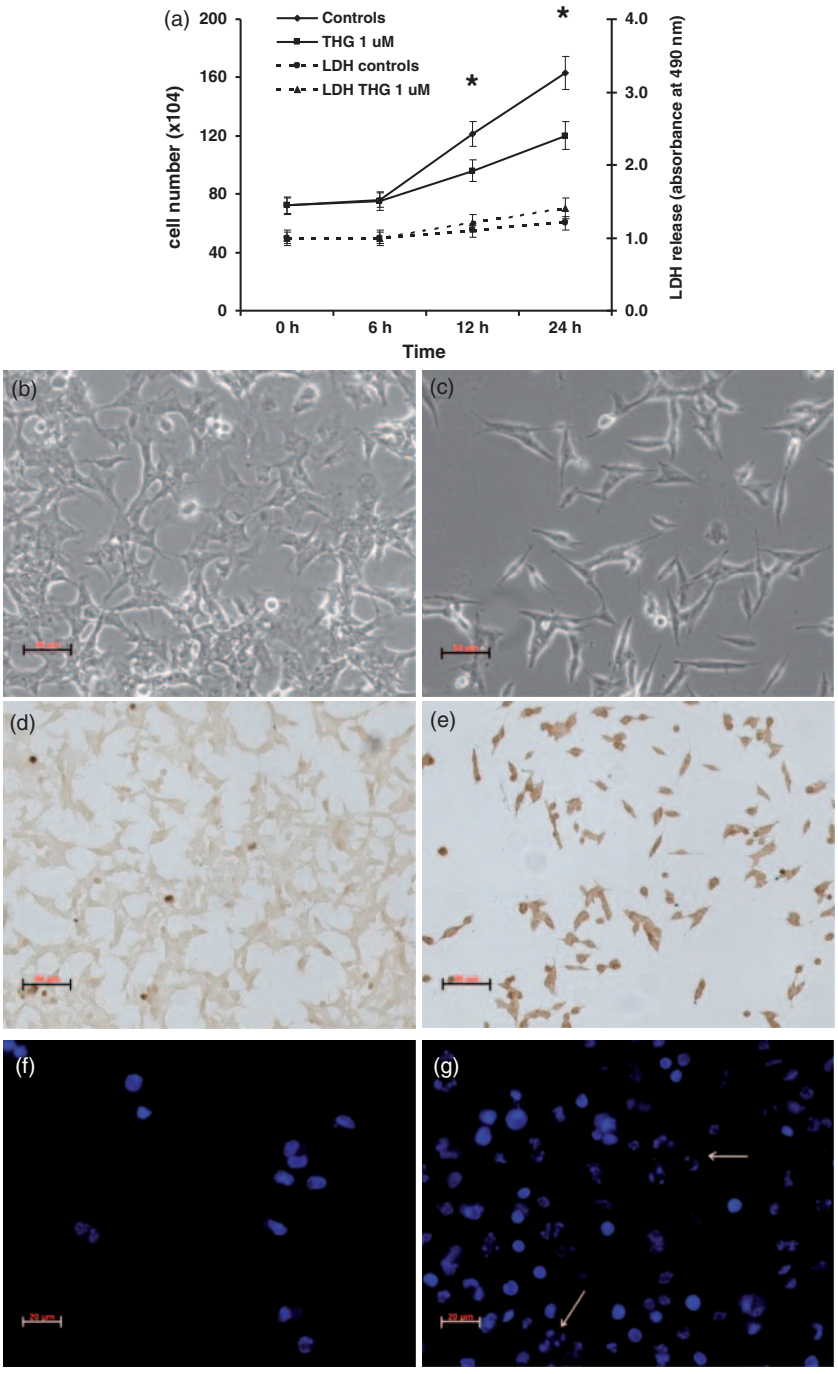

Figure 2 (a) Effect of THG on the growth of SK-N-BE cells. Cells were initially seeded at the density of $10^4 \times cm^2$ on 60-mm plastic culture dishes and were grown for 48 h in a CO_2 incubator. At each endpoint of treatment selected, cells were harvested, and the cell number per dish was counted in a haematocytometer chamber. As shown, 1 μM THG induced a significant progressive reduction in the adherent cell number, with respect to the untreated cells. At the same time, THG-treated cells showed also a modest and not significant increase in LDH released in the culture medium with respect to untreated cells. The means and SEM of six separate experiments are represented. *$P < 0.05$ versus untreated cells. (b and c) Effect of THG on the morphology of SK-N-BE cells. Phase contrast microphotographs of (b) untreated and (c) cells treated for 24 h with 1 μM THG. Control cells displayed a homogeneous cytosol and the emission of several cell processes, while 24 h of 1 μM THG treatment resulted in a loss of neuritis, cell texture and shape, and a decrease in cell number, with respect to controls. Representative results of five independent experiments are shown. (d to g) THG induces apoptosis in SK-N-BE cells. Evaluation of apoptosis in adherent (d) control cells, and (e) cells treated for 24 h with 1 μM THG, using the TUNEL assay. Remarkable positivity for TUNEL staining, as a result of chromatin fragmentation, was clearly evident in THG-treated cells, in which a consistent reduction in cell number was also apparent, in comparison to controls. Evaluation of apoptosis in cells collected from the supernatants of (f) controls, and (g) cells treated for 24 h with 1 μM THG, using DAPI staining. Apoptotic, fragmented nuclei were detectable from supernatants of THG-treated cells, in which chromatin clumps as well as condensed nuclei with aggregated chromatin were visible (arrows). Note that the number of detached cells was higher in THG-treated cells compared with controls. Typical experimental results of five independent experiments are shown. Bars: b–e = 50 μm; f, g = 20 μm. (A color version of this figure is available in the online journal.)

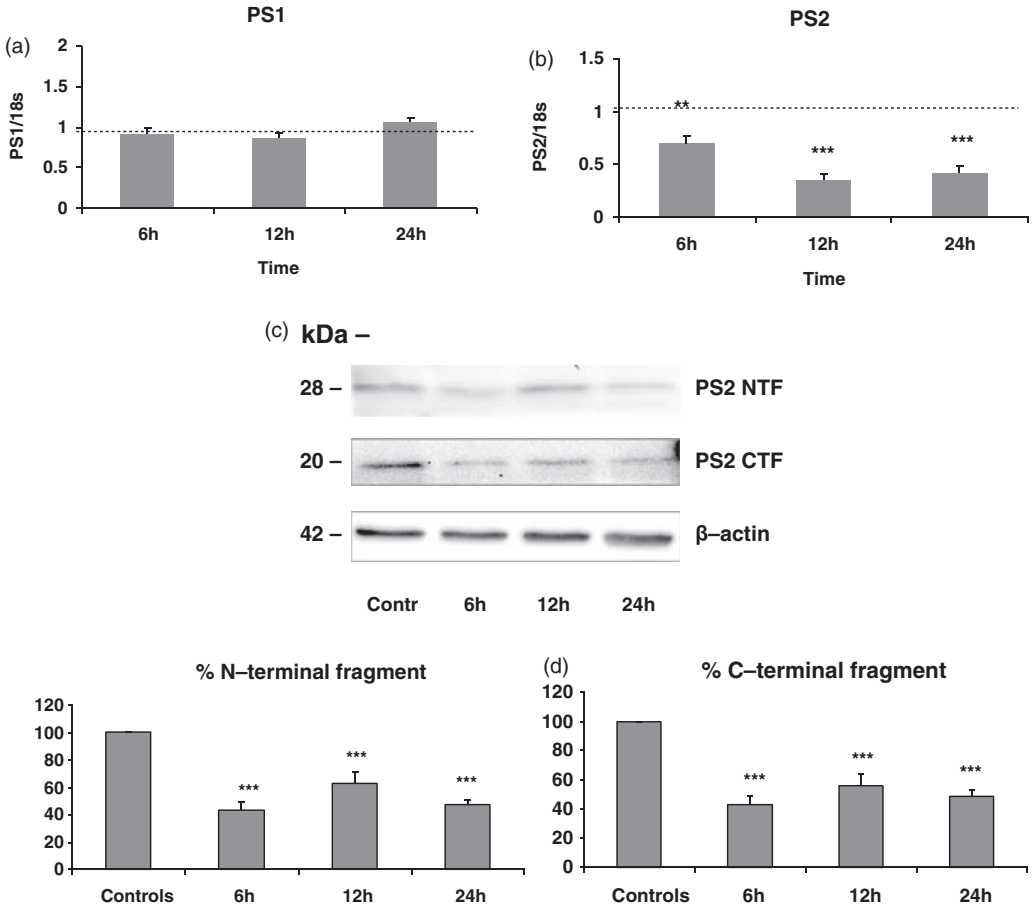

Figure 3 (a and b) Time-related PS1 and PS2 gene expression induced by THG. Expression levels of (a) PS1 and (b) PS2 were analyzed by RT-qPCR in SK-N-BE cells treated with 1 μM THG for up to 24 h. The data, compared to 18 S rRNA, were expressed as fold changes relative to the control at each treatment time. The mean ± SEM of five experiments is shown. $^{**}P < 0.01$, $^{***}P < 0.001$ versus untreated cells. (c and d) Time-related PS2 protein expression changes induced by THG. (c) On the left: representative Western blot showing the effects of treatment with 1 μM THG for up to 24 h in SK-N-BE cells; on the right: statistical data of blot densitometry of the bands corresponding to PS2 (mean values ± SEM $n = 4$). Cell lysates (20 μg per lane) were loaded on 10% denaturing gel and immunoblotted as reported in material and methods. $^{***}P < 0.001$ versus untreated cells

THG-induced cell-growth arrest is associated with a time-dependent emerging pro-oxidant condition

Cerella *et al.*[48] reported that the apoptogenic activity of THG in U937 cells can be modulated by the cellular redox state. To determine whether the THG-induced apoptosis was associated with oxidative stress in our experimental model, a time-dependent investigation into the redox profile of SK-N-BE cells was carried out. Incubation of cells with 1 μM THG resulted in a 3.3-, 2-, and 1.87-fold increase in SOD activity, evaluated respectively at 6, 12, and 24 h of THG exposure (Figure 4(a)). In view of these effects and given the role of GSH as one of the most important intracellular defenses against oxidative damage, a specific analysis of the effect of 1 μM THG on intracellular GSH and GSSG levels was carried out by exposing SK-N-BE cells for various periods up to 24 h. The results showed that 6 h of THG treatment did not introduce any GSH perturbations. However, 12 h of THG exposure induced a 19% drop in GSH concentration and a 2.5-fold increase in the GSSG level. Finally, after 24 h of THG treatment, the GSH content dropped to a minimum of 35%, and GSSG increased 2.8-fold with respect to the untreated cells (Figure 4(b) to (d)).

Manipulation of the internal redox profile does not reverse the effect of THG on SK-N-BE cells

To address the question of whether the basal GSH pool is critical for THG-induced cell-growth arrest, experiments in which the GSH/GSSG ratio was manipulated before subsequent THG exposure were performed. For this purpose, SK-N-BE neuron-like cells were pretreated for 24 h with the pro-oxidant and GSH-depleting agent BSO (100 μM) or for 4 h with the antioxidant and thiol supplier NAC (5 mM). Then, cell monolayers were exposed for 24 h to 1 μM THG. As shown in Figure 5(a), neither BSO nor NAC was able to reverse the cell-growth arrest induced by THG treatment, although a partial recovery of cell number was apparent in BSO pretreated cells. Moreover, neither BSO nor NAC pretreatment had any effect on the GSH/GSSG ratio with respect to that reported for THG alone (Figure 5(b)). As shown in Figure 5(c) and (d), the different redox profiles

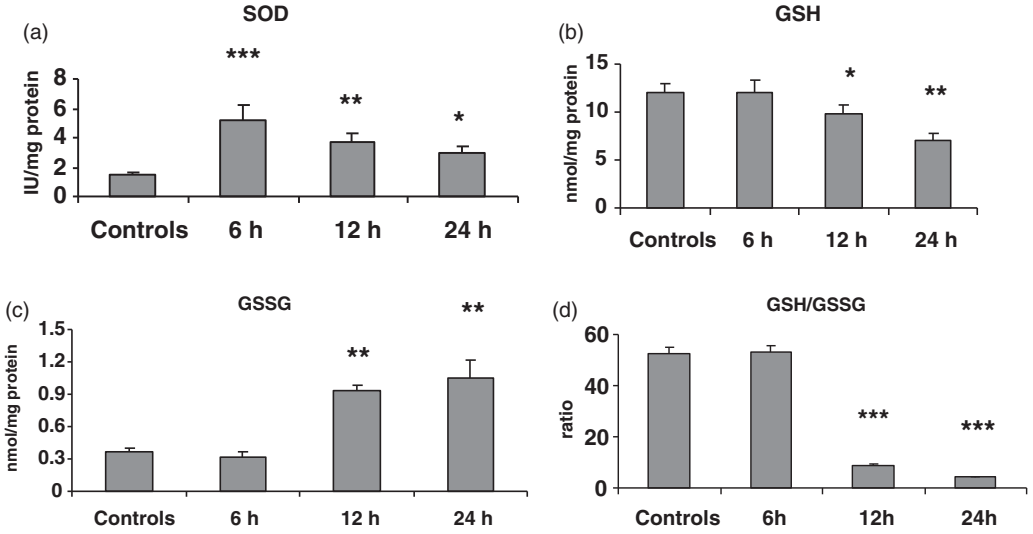

Figure 4 Time-related oxidative stress changes induced by THG in SK-N-BE cells. THG treatment induced a time-dependent alteration in the redox profile of the cells, particularly in SOD activity (a), GSH (b), and GSSG (c) contents, with a progressive net reduction in the GSH/GSSG ratio (d). The mean ± SEM of five experiments are shown. $^{*}P < 0.05$, $^{**}P < 0.01$, and $^{***}P < 0.001$ versus untreated cells

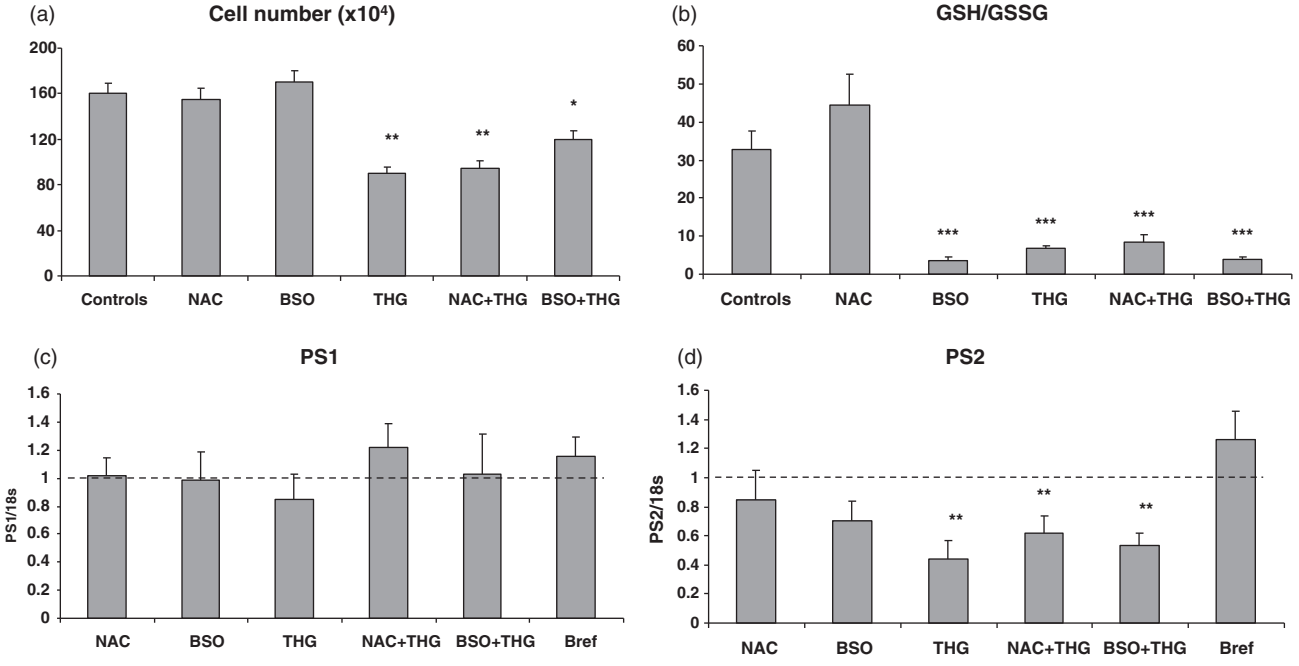

Figure 5 (a and b) Effects of BSO and NAC pretreatments on THG-induced cell-growth arrest and apoptosis and GSH/GSSG ratio. Subconfluent SK-N-BE cells were pretreated for 24 h with 100 μM BSO (24 h) or for 2 h with 5 mM NAC. Then, 1 μM THG was added to the cell cultures for 24 h. As shown, the different redox profiles induced by BSO and NAC pretreatments did not sensitize SK-N-BE cells to THG-induced cell-growth arrest and did not alter the GSH/GSSG ratio with respect to that reported for THG alone. (c and d) Different redox profiles of the cells do not reverse the PS2 down-regulation induced by THG, while Ca^{2+}-independent ER stress does not modify PS1 and PS2 expression. The different redox profiles induced by BSO and NAC pretreatments did not affect the (c) PS1 and (d) PS2 gene expression detected after 24 h THG treatment in SK-N-BE cells. Additional experiments with 5 μg/mL Brefeldin A, a well-known ER perturbing agent that does not induce Ca^{2+} mobilization, were carried out. As shown, Brefeldin A did not affect either (c) PS1 or (d) PS2 transcriptional activity. $n = 5$, $^{*}P < 0.05$, $^{**}P < 0.01$, and $^{***}P < 0.001$ versus untreated cells

induced by BSO (pro-oxidant environment) or NAC (anti-oxidant environment) pretreatment did not modify *per se* either PS1 or PS2 gene expression. This is in keeping with the lack of involvement of oxidative stress in PS2 down-regulation. Finally, neither of the redox manipulations was able to reverse the reported PS2 down-regulation detected after 24 h of 1 μM THG exposure (Figure 5(d)).

Brefeldin A does not modulate PS expression in SK-N-BE cells

As THG is well-known Ca^{2+} mobilizator and ER-stress agent, and in order to solve the question if the reported PS2 down-regulation depended on Ca^{2+} mobilization only or the involvement of other paradigm may be considered;

specific experiments with Brefeldin A (5 μg/mL), a Ca^{2+}-independent ER stressor, were carried out. As can be observed in Figure 5(c) and (d), Brefeldin A did not significantly modify basal PS1 and PS2 gene expression.

Discussion

Intracellular Ca^{2+} signaling is fundamental to neuronal physiology and pathophysiology. Because of its complex and ubiquitous roles, the disruption of Ca^{2+} homeostasis is implicated in various multifactorial neurodegenerative diseases such as AD. So far, the underlying pathogenic mechanisms of AD have remained obscure. However, a body of evidence suggests that sustained disruption of intracellular Ca^{2+} signaling may play an early, and perhaps central, role in AD pathogenesis.[49–56]

It has been documented that PS1 and PS2 are expressed at comparable levels in the human brain, and that they change as a function of age, with PS1 being expressed at a higher level in the developing brain, and PS2 during postnatal development.[57] This suggests that PSs are subject to physiologically differential transcriptional regulation during brain maturation. PSs are also differentially regulated during brain damage and neurodegeneration. In fact, a significant decrease in PS2 mRNA was observed in the pathologically affected areas of late-onset SAD brains.[18,58] Moreover, it has also been reported that the decrease in PS2 expression is as severe in subjects with mild AD as it is in subjects in later stages of the disease, suggesting that the down-regulation of PS2 gene expression appears to be an early event in sporadic late-onset AD.[19] Currently, there is little information about the factors that influence and control PS2 expression, but understanding PS2 regulation could be important for elucidating its role in AD.

Deranged Ca^{2+} signaling is a critical event for apoptosis.[59] Transient and sustained elevation of cytosolic and mitochondrial Ca^{2+} may start a chain of biochemical events leading to apoptosis, such as opening of the mitochondrial permeability transition pores, mitochondrial membrane potential collapse,[60] oxidative stress,[61] the release of apoptogenic factors, and cell death.[62] We wondered whether the reported PS2 down-regulation was also dependent on Ca^{2+} mobilization. To answer this question, we used a Ca^{2+} mobilizer that is known to deplete ER Ca^{2+} by inhibiting SERCA, as confirmed in our SK-N-BE cells in videoimaging experiments, which showed the complete depletion of ER Ca^{2+} and an increase in the cytoplasmic basal Ca^{2+} level in THG-treated cells.[63] When we treated the neuroblastoma cell line with THG, we observed that release of Ca^{2+} from the ER was able to induce up to 65% down-regulation of PS2 mRNA in our cell model, while its homolog, PS1, was not affected by the treatment. Interestingly, the extent of PS2 mRNA down-regulation, as observed in our cell model, was in line with that described by McMillian *et al.*[58] and Takami *et al.*[18], in different areas of AD affected brains. Furthermore, the consistent and significant decreased level of both NTF and CTF suggest that Ca^{2+} imbalance also has a role in the increased proteolytic turnover of both fragments.

There is a growing interest in the study of the relationship between ER Ca^{2+} depletion and apoptosis. Moreover, some authors have reported that reticular stress is implicated in apoptotic neuronal cell death occurring in AD.[64,65] THG is a ER-stress agent known to induce the apoptotic machinery in several cell models.[66,67] As expected, we found that THG caused apoptotic cell death in a human neuroblastoma cell line in parallel with a consistent increase in the concentration of Ca^{2+} in the cytosol. As previously discussed, this cell death feature is accompanied by the significant progressive down-regulation of PS2 but not PS1, suggesting that, despite their strong structural homology, PS1 and PS2 may have different functions[68–71] and regulatory pathways. The parallel use of Brefeldin A, an ER stressor agent that acts without affecting Ca^{2+} homeostasis, allowed us to verify that probably only the rise in cytosolic Ca^{2+} is able to affect both PS2 gene and protein expression, while ER stress *per se* does not appear to be involved in this event.

As it has previously been demonstrated that the PS2 promoter contains several potential binding sites for nuclear transcription factors that are sensitive to the redox status of the cells,[72] we addressed the question of whether the redox balance might modulate the sensitivity of cells to the apoptotic stimulus induced by THG. We found that altering the basal level of GSH, the main soluble intracellular antioxidant, had no effect on either PS2 down-regulation or apoptosis induced by THG treatment. This suggests that THG exerts a dominant effect, which overcome all the thiol redox manipulations performed (i.e., NAC and BSO treatments). Thus, although the involvement of oxidative stress in THG-induced apoptosis cannot be completely ruled out, these data suggest that the imbalance of redox homeostasis within the cell probably has only a secondary role in the cell death process triggered by THG treatment in our experimental setting, and does not influence PS2 expression.

Given that (1) THG exerts its Ca^{2+} deregulatory activity via an irreversible inhibitory effect on SERCA pumps, thus inhibiting the Ca^{2+} influx within ER, and that (2) PS2 endoproteolytic fragments have been found to interact directly via sorcin with RyRs and IP3Rs,[16,17,73] we hypothesize that the observed PS2 drop of both NTF and CTF which follows THG exposure could be a type of adaptive response evoked by the cells to counteract the increased presence of Ca^{2+} within the cytosol.

As reported by other authors,[74] PS2 may directly participate, with a regulatory role, in the biochemical cascade leading to apoptosis. Thus, in view of the reported capability of both wild-type and mutated PS2 to induce p53-dependent apoptosis,[75] and the demonstration that the transfection of antisense PS2 confers protection against apoptosis,[76] we suggest that in our experimental setting cells could be attempting to reverse the process of apoptotic cell death by down-regulating PS2 expression. Our data concerning the association of PS2 down-regulation with the occurrence of apoptosis in neuron-like cells support the hypothesis of possible PS2 involvement in the same pathological pathways leading to sporadic AD.

In conclusion, in our *in vi*tro experimental model, Ca^{2+} fluctuation rather than ER stress and/or oxidative

imbalance seems to play an essential role in PS2 regulation. These findings are in line with those reported recently by our group showing that, beside a significant PS down-regulation, 24 h of 1 μM THG increased by 400% the $A\beta_{1-42}$ peptide concentration in the medium of the H4 human neuroglioma cell line stably transfected with the Swedish double mutation.[40] These results seem to suggest that Ca^{2+} deregulation may be an important modulating factor for Aβ production in neuronal cells via PS down-regulation. Moreover, as the $A\beta_{1-42}$ peptide itself is a well-known pro-apoptotic agent which alters the intracellular Ca^{2+} equilibrium, a possible loop mechanism involving disruption of Ca^{2+} homeostasis, apoptosis, and alterations in APP processing may be postulated.[9] The real linkage between PS2 and other proteins that are involved in Ca^{2+} handling remains to be established and requires further specific studies. In fact, given the complexity of cellular Ca^{2+} homeostasis, with its several pools and many regulatory steps, there is a need for additional investigations to dissect the way(s) in which PS influences the capability of neurons to handle intracellular calcium.

Author contributions: All authors have made significant scientific contributions to the study. They are thoroughly familiar with the primary data and have reviewed the manuscript. RR, SV, PP, AC, and AC designed the study; RR, PP, CDN, AC, PR, and FS conducted the experiments; SV and CDN supplied critical expertise in the field of calcium analysis; RR, SV, PP, AC, and AC analyzed the primary data and wrote the manuscript.

ACKNOWLEDGEMENTS

This study was supported by a grant from the Italian Ministry of Health: ''Genetic determinants and modulator factors in neurodegenerative diseases: clinical and experimental model'' to AC.

REFERENCES

1. Selkoe DJ. Alzheimer's disease: genes, proteins, and therapy. *Physiol Rev* 2001;**81**:741–66
2. Dickson DW. Neuropathological diagnosis of Alzheimer's disease: a perspective from longitudinal clinicopathological studies. *Neurobiol Aging* 1997;**18**:S21–6
3. Verdile G, Fuller S, Atwood CS, Laws SM, Gandy SE, Martins RN. The role of beta amyloid in Alzheimer's disease: still a cause of everything or the only one who got caught? *Pharmacol Res* 2004;**50**:397–409
4. Walter J, Kaether C, Steiner H, Haass C. The cell biology of Alzheimer's disease: uncovering the secrets of secretases. *Curr Opin Neurobiol* 2001;**11**:585–90
5. Smolarkiewicz M, Skrzypczak T, Wojtaszek P. The very many faces of presenilins and γ-secretase complex. *Protoplasma* 2013;**250**:997–1011
6. Cowburn RF, Popescu BO, Ankarcrona M, Dehvari N, Cedazo-Minguez A. Presenilin-mediated signal transduction. *Physiol Behav* 2007;**92**:93–7
7. Lippa CF, Saunders AM, Smith TW, Swearer JM, Drachman DA, Ghetti B, Nee L, Pulaski-Salo D, Dickson D, Robitaille Y, Bergeron C, Crain B, Benson MD, Farlow M, Hyman BT, George-Hyslop SP, Roses AD, Pollen DA. Familial and sporadic Alzheimer's disease: neuropathology cannot exclude a final common pathway. *Neurology* 1996;**46**:406–12
8. Green KH, LaFerla FM. Linking calcium to Aβ and Alzheimer's disease. *Neuron* 2008;**59**:190–4
9. Bojarski L, Herms J, Kuznicki J. Calcium dysregulation in Alzheimer's disease. *Neurochem Int* 2008;**52**:621–33
10. Lee SY, Hwang DY, Kim YK, Lee JW, Shin IC, Oh KW, Lee MK, Lim JS, Yoon DY, Hwang SJ, Hong JT. PS2 mutation increases neuronal cell vulnerability to neurotoxicants through activation of caspase-3 by enhancing of ryanodine receptor-mediated calcium release. *FASEB J* 2006;**20**:151–3
11. Cheung KH, Shineman D, Müller M, Cárdenas C, Mei L, Yang J, Tomita T, Iwatsubo T, Lee VM, Foskett JK. Mechanism of Ca^{2+} disruption in Alzheimer's disease by presenilin regulation of InsP3 receptor channel gating. *Neuron* 2008;**58**:871–83
12. Green KN, Demuro A, Akbari Y, Hitt BD, Smith IF, Parker I, LaFerla FM. SERCA pump activity is physiologically regulated by presenilin and regulates amyloid beta production. *J Cell Biol* 2008;**181**:1107–16
13. Brunello L, Zampese E, Florean C, Pozzan T, Pizzo P, Fasolato C. Presenilin-2 dampens intracellular Ca^{2+} store by increasing Ca^{2+} leakage and reducing Ca^{2+} uptake. *J Cell Mol Med* 2009;**13**:3358–69
14. Zhang H, Sun S, Herreman A, De Strooper B, Bezprozvanny I. Role of presenilins in neuronal calcium homeostasis. *J Neurosci* 2010;**23**:8566–80
15. Honarnejad K, Herms J. Presenilins: role in calcium homeostasis. *Int J Biochem Cell Biol* 2012;**44**:1983–6
16. Takeda T, Asahi M, Yamaguchi O, Hikoso S, Nakayama H, Kusakari Y, Kawai M, Hongo K, Higuchi Y, Kashiwase K, Watanabe T, Taniike M, Nakai A, Nishida K, Kurihara S, Donoviel DB, Bernstein A, Tomita T, Iwatsubo T, Hori M, Otsu K. Presenilin 2 regulates the systolic function of heart by modulating Ca^{2+} signalling. *FASEB J* 2005;**19**:2069–71
17. Cai C, Lin P, Cheung KH, Li N, Levchook C, Pan Z, Ferrante C, Boulianne GL, Foskett JK, Danielpour D, Ma J. The presenilin-2 loop peptide perturbs intracellular Ca^{2+} homeostasis and accelerates apoptosis. *J Biol Chem* 2006;**281**:16649–55
18. Takami K, Terai K, Matsuo A, Walker DG, McGeer PL. Expression of presenilin-1 and -2 mRNAs in rat and Alzheimer's disease brains. *Brain Res* 1997;**748**:122–30
19. McMillan PJ, Leverenz JB, Dorsa DM. Specific downregulation of presenilin 2 gene expression is prominent during early stages of sporadic late-onset Alzheimer's disease. *Brain Res Mol Brain Res* 2000;**78**:138–45
20. Nishiyama K, Murayama S, Suzuki T, Mitsui Y, Sakaki Y, Kanazawa I. Presenilin 1 mRNA expression in hippocampi of sporadic Alzheimer's disease patients. *Neurosci Res* 1996;**26**:75–8
21. Maccioni RB, Muñoz JP, Barbeito L. The molecular bases of Alzheimer's disease and other neurodegenerative disorders. *Arch Med Res* 2001;**32**:367–81
22. Greenfield JP, Tsai J, Gouras GK, Hai B, Thinakaran G, Checler F, Sisodia SS, Greengard P, Xu H. Endoplasmic reticulum and trans-Golgi network generate distinct populations of Alzheimer β-amyloid peptides. *Proc Natl Acad Sci U S A* 1999;**96**:742–7
23. Cook DG, Forman MS, Sung JC, Leight S, Kolson DL, Iwatsubo T, Lee VM, Doms RW. Alzheimer's A beta(1-42) is generated in the endoplasmic reticulum/intermediate compartment of NT2N cells. *Nat Med* 1997;**3**:1021–3
24. Haass C. Presenilins: genes for life and death. *Neuron* 1997;**18**:687–90
25. Doan A, Thinakaran G, Borchelt DR, Slint HH, Ratovitski T, Podlisny M, Selkoe DJ, Seeger M, Gandy SE, Price DL, Sisodia SS. Protein topology of presenilin 1. *Neuron* 1996;**17**:1023–30
26. Mattson MP. ER calcium and Alzheimer's disease: in a state of flux. *Sci Signal* 2010;**3**:10
27. Sasaki S. Endoplasmic reticulum stress in motor neurons of the spinal cord in sporadic amyotrophic lateral sclerosis. *J Neuropathol Exp Neurol* 2010;**69**:346–55
28. Soto C. Endoplasmic reticulum stress, PrP trafficking, and neurodegeneration. *Dev Cell* 2008;**15**:339–41
29. Chafekar SM, Zwart R, Veerhuis R, Vanderstichele H, Baas F, Scheper W. Increased Abeta1-42 production sensitizes neuroblastoma cells for ER stress toxicity. *Curr Alzheimer Res* 2008;**5**:469–74
30. Resende R, Ferreiro E, Pereira C, Resende de Oliveira C. Neurotoxic effect of oligomeric and fibrillar species of amyloid-beta peptide 1-42: involvement of endoplasmic reticulum calcium release in oligomer-induced cell death. *Neuroscience* 2008;**115**:725–37

31. Katayama T, Imaizumi K, Manabe T, Hitomi J, Kudo T, Tohyama M. Induction of neuronal death by ER stress in Alzheimer's disease. *J Chem Neuroanat* 2004;**28**:67–78
32. Dröge W, Scipper HM. Oxidative stress and aberrant signaling in aging and cognitive decline. *Aging Cell* 2007;**6**:361–70
33. Serrano F, Klann E. Reactive oxygen species and synaptic plasticity in the aging hippocampus. *Ageing Res Rev* 2004;**3**:431–43
34. Toescu EC, Verkhratsky A. Neuronal ageing from an intraneuronal perspective: roles of endoplasmic reticulum and mitochondria. *Cell Calcium* 2003;**34**:311–23
35. Tabaton M, Tamagno E. The molecular link between beta- and gamma-secretase activity on the amyloid beta precursor protein. *Cell Mol Life Sci* 2007;**64**:2211–18
36. Thastrup O, Cullen PJ, Drøbak BK, Hanley MR, Dawson AP. Thapsigargin, a tumor promoter, discharges intracellular Ca^{2+} stores by specific inhibition of the endoplasmic reticulum Ca^{2+}-ATPase. *Proc Natl Acad Sci U S A* 1990;**87**:2466–70
37. Copanaki E, Schürmann T, Eckert A, Leuner K, Müller WE, Prehn JH, Kögel D. The amyloid precursor protein potentiates CHOP induction and cell death in response to ER Ca^{2+} depletion. *Biochim Biophys Acta* 2007;**1773**:157–65
38. Jin H, Sanjo N, Uchihara T, Watabe K, St George-Hyslop P, Fraser PE, Mizusawa H. Presenilin-1 holoprotein is an interacting partner of sarco endoplasmic reticulum calcium-ATPase and confers resistance to endoplasmic reticulum stress. *J Alzheimers Dis* 2010;**20**:261–73
39. Crestini A, Piscopo P, Iazeolla M, Albani D, Rivabene R, Forloni G, Confaloni A. Rosuvastatin and thapsigargin modulate γ-Secretase gene expression and APP processing in a human neuroglioma model. *J Mol Neurosci* 2011;**89**:276–83
40. Werno C, Zhou J, Brüne B. A23187, ionomycin and thapsigargin upregulate mRNA of HIF-1alpha via endoplasmic reticulum stress rather than a rise in intracellular calcium. *J Cell Physiol* 2008;**215**:708–14
41. Becker A, Soliman KF. The role of intracellular glutathione in inorganic mercury-induced toxicity inneuroblastoma cells. *Neurochem Res* 2009;**34**:1677–84
42. Shimizu E, Hashimoto K, Komatsu N, Iyo M. Roles of endogenous glutathione levels on 6-hydroxydopamine-induced apoptotic neuronal cell death in human neuroblastoma SK-N-SH cells. *Neuropharmacology* 2002;**43**:434–43
43. Marklund S, Marklund G. Involvement of the superoxide anion radical in the autoxidation of pyrogallol and a convenient assay for superoxide dismutase. *Eur J Biochem* 1974;**47**:469–74
44. Anderson ME. Determination of glutathione and glutathione disulfide in biological samples. *Methods Enzymol* 1985;**113**:548–55
45. Lee H, Choi BH, Suh BC, Lee SK, Kim KT. Attenuation of signal flow from P2Y6 receptor by protein kinase C-alpha in SK-N-BE(2)C human neuroblastoma cells. *J Neurochem* 2003;**85**:1043–53
46. Thinakaran G, Borchelt DR, Lee MK, Slunt HH, Spitzer L, Kim G, Ratovitsky T, Davenport F, Nordstedt C, Seeger M, Hardy J, Levey AI, Gandy SE, Jenkins NA, Copeland NG, Price DL, Sisodia SS. Endoproteolysis of presenilin 1 and accumulation of processed derivatives in vivo. *Neuron* 1996;**17**:181–90
47. Honarnejad K, Jung CK, Lammich S, Arzberger T, Kretzschmar H, Herms J. Involvement of presenilin holoprotein upregulation in calcium dyshomeostasis of Alzheimer's disease. *J Cell Mol Med* 2013;**17**:293–302
48. Cerella C, Coppola S, D'Alessio M, De Nicola M, Magrini A, Bergamaschi A, Ghibelli L. Redox modulation of the apoptogenic activity of thapsigargin. *Ann N Y Acad Sci* 2007;**1099**:469–72
49. Gandy S, Doeven MK, Poolman B. Alzheimer disease: presenilin springs a leak. *Nat Med* 2006;**12**:1121–3
50. LaFerla FM. Calcium dyshomeostasis and intracellular signalling in Alzheimer's disease. *Nat Rev Neurosci* 2002;**3**:862–72
51. Mattson MP, Chan SL. Neuronal and glial calcium signaling in Alzheimer's disease. *Cell Calcium* 2003;**34**:385–97
52. Smith IF, Green KN, LaFerla FM. Calcium dysregulation in Alzheimer's disease: recent advances gained from genetically modified animals. *Cell Calcium* 2005;**38**:427–37
53. Stutzmann GE. Calcium dysregulation, IP3 signaling, and Alzheimer's disease. *Neuroscientist* 2005;**11**:110–15
54. Camandola S, Mattson MP. Aberrant subcellular neuronal calcium regulation in aging and Alzheimer's disease. *Biochim Biophys Acta* 2011;**1813**:965–73
55. Supnet C, Bezprozvanny I. The dysregulation of intracellular calcium in Alzheimer disease. *Cell Calcium* 2010;**47**:183–9
56. Woods NK, Padmanabhan J. Neuronal calcium signaling and Alzheimer's disease. *Adv Exp Med Bio* 2012;**740**:1193–217
57. Lee MK, Slunt HH, Martin LJ, Thinakaran G, Kim G, Gandy SE, Seeger M, Koo E, Price DL, Sisodia SS. Expression of presenilin 1 and 2 (PS1 and PS2) in human and murine tissues. *J Neurosci* 1996;**16**:7513–25
58. McMillan PJ, Leverenz JB, Poorkaj P, Schellenberg GD, Dorsa DM. Neuronal expression of STM2 mRNA in human brain is reduced in Alzheimer's disease. *J Histochem Cytochem* 1996;**44**:1215–22
59. Rizzuto R, Pinton P, Ferrari D, Chami M, Szabadkai G, Magalhães PJ, Di Virgilio F, Pozzan T. Calcium and apoptosis: facts and hypotheses. *Oncogene* 2003;**22**:8619–927
60. Tornero D, Ceña V, González-García C, Jordán J. The role of the mitochondrial permeability transition pore in neurodegenerative processes. *Rev Neurol* 2002;**35**:354–61
61. Shi Q, Gibson GE. Oxidative stress and transcriptional regulation in Alzheimer disease. *Alzheimer Dis Assoc Disord* 2007;**21**:276–91
62. Zoratti M, Szabò I. The mitochondrial permeability transition. *Biochim Biophys Acta* 1995;**1241**:139–76
63. Lytton J, Westlin M, Hanley MR. Thapsigargin inhibits the sarcoplasmic or endoplasmic reticulum Ca-ATPase family of calcium pumps. *J Biol Chem* 1991;**266**:17067–71
64. Paschen W, Frandsen A. Endoplasmic reticulum dysfunction–a common denominator for cell injury in acute and degenerative diseases of the brain? *J Neurochem* 2001;**79**:719–25
65. Paschen W. Dependence of vital cell function on endoplasmic reticulum calcium levels: implications for the mechanisms underlying neuronal cell injury in different pathological states. *Cell Calcium* 2001;**29**:1–11
66. Nguyen HN, Wang C, Perry DC. Depletion of intracellular calcium stores is toxic to SH-SY5Y neuronal cells. *Brain Res* 2002;**924**:159–66
67. Arias E, Alés E, Gabilan NH, Cano-Abad MF, Villarroya M, García AG, López MG. Galantamine prevents apoptosis induced by beta-amyloid and thapsigargin: involvement of nicotinic acetylcholine receptors. *Neuropharmacology* 2004;**46**:103–14
68. Lai MT, Chen E, Crouthamel MC, DiMuzio-Mower J, Xu M, Huang Q, Price E, Register RB, Shi XP, Donoviel DB, Bernstein A, Hazuda D, Gardell SJ, Li YM. Presenilin-1 and presenilin-2 exhibit distinct yet overlapping gamma-secretase activities. *J Biol Chem* 2003;**278**:22475–81
69. Mastrangelo P, Mathews PM, Chishti MA, Schmidt SD, Gu Y, Yang J, Mazzella MJ, Coomaraswamy J, Horne P, Strome B, Pelly H, Levesque G, Ebeling C, Jiang Y, Nixon RA, Rozmahel R, Fraser PE, St George-Hyslop P, Carlson GA, Westaway D. Dissociated phenotypes in presenilin transgenic mice define functionally distinct gamma-secretases. *Proc Natl Acad Sci U S A* 2005;**102**:8972–7
70. Verdile G, Gandy SE, Martins RN. The role of presenilin and its interacting proteins in the biogenesis of Alzheimer's beta amyloid. *Neurochem Res* 2007;**32**:609–23
71. Zampese E, Fasolato C, Kipanyula MJ, Bortolozzi M, Pozzan T, Pizzo P. Presenilin 2 modulates endoplasmic reticulum (ER)-mitochondria interactions and Ca^{2+} cross-talk. *Proc Natl Acad Sci U S A* 2001;**108**:2777–82
72. Pennypacker KR, Fuldner R, Xu R, Hernandez H, Dawbarn D, Mehta N, Perez-Tur J, Baker M, Hutton M. Cloning and characterization of the presenilin-2 gene promoter. *Brain Res Mol Brain Res* 1998;**56**:57–65
73. Pack-Chung E, Meyers MB, Pettingell WP, Moir RD, Brownawell AM, Cheng I, Tanzi RE, Kim TW. Presenilin 2 interacts with sorcin, a modulator of the ryanodine receptor. *J Biol Chem* 2000;**275**:14440–5
74. Ghidoni R, Gasparini L, Alberici A, Benussi L, Barbiero L, Mazzoli F, Nicosia F, Finazzi D, Benerini Gatta L, Albertini A, Zanetti O, Binetti G. Inhibition of energy metabolism down-regulates the Alzheimer related presenilin 2 gene. *J Neural Transm* 2003;**110**:1029–39

75. Alves da Costa C, Paitel E, Mattson MP, Amson R, Telerman A, Ancolio K, Checler F. Wild-type and mutated presenilins 2 trigger p53-dependent apoptosis and down-regulate presenilin 1 expression in HEK293 human cells and in murine neurons. *Proc Natl Acad Sci U S A* 2002;**99**:4043–8
76. Wolozin B, Iwasaki K, Vito P, Ganjei JK, Lacanà E, Sunderland T, Zhao B, Kusiak JW, Wasco W, D'Adamio L. Participation of presenilin 2 in apoptosis: enhanced basal activity conferred by an Alzheimer mutation. *Science* 1996;**274**:1710–13

(Received June 11, 2013, Accepted October 15, 2013)